DOI: 10.12731/2658-6649-2025-17-2-1295 **EDN: RZPONV**
UDC 547.78:577.16:615.4:615.9

Original article

THE ECO-FREIENDLY SYNTHESIS OF SILVER NANOPARTICLES (AgNPs) USING MARANTA LEUCONEURA ETHANOLIC EXTRACT WITH THE ASSESSMENT OF ANTIBACTERIAL, ANTIOXIDANT, ANTICANCER ACTIVITIES

N.M. Alassadi, G.J. Al-Ghizzawi

Abstract

Background. Considering the significant interest in the use of biosynthesized silver nanoparticles (AgNPs) obtained from plant extracts.

Purpose. The study is aimed to utilize the ethanolic extract of Maranta leuconeura as a reducing agent to form AgNPs, and evaluate its biological potential effect.

Materials and methods. The plant was extracted using 70% ethanol to create silver nanoparticles.The synthesis of AgNPs was initially confirmed by surface plasmon resonance at 400 nm, facilitated by biologically active compounds that contributed to reduction, capping, and stabilization, as evidenced by FTIR analysis, while zeta potential analysis indicated good stability at -37.1 mV. The fabricated AgNPs microscopic study revealed spherical particles of average sizes 39.9 nm, whereas XRD analysis indicated a face-centred cubic (FCC) crystalline nature.

Results and discussion. The antibacterial efficacy of AgNPs against tested isolates indicated that *Staphylococcus epidermidis* and *Proteus mirabilis* exhibited the highest sensitivity to silver nanoparticles, with an average inhibition zone measuring 14.4 mm. The results of the antioxidant activity demonstrated comparable radical scavenging to ascorbic acid, depending on the concentration. The evaluation of cytotoxicity against cancer SiHa cell line and normal HdFn cell line, revealed a concentration-dependent effect and potential anticancer impact, with an IC_{50} of 17.49 and 125 μg/ml for SiHa and HdFn respectively.

Conclusion. Nanoparticles produced from *Maranta leuconeura* leaf extract may be significant in medicinal applications owing to their distinctive features.

Keywords: AgNPs; Maranta leuconeura; antibacterial activity; SiHa; antioxidant activity

For citation. Alassadi, N. M., & Al-Ghizzawi, G. J. (2025). The eco-friendly synthesis of silver nanoparticles (AgNPs) using Maranta leuconeura ethanolic extract with the assessment of antibacterial, antioxidant, anticancer activities. *Siberian Journal of Life Sciences and Agriculture*, *17*(2), 217-236. https://doi.org/10.12731/2658-6649-2025-17-2-1295

Introduction

The characteristics of nanoparticles (NPs), when contrasted with their bulk counterparts, confer significant importance upon them. According to [1], nanomaterials display many features, such as biological, magnetic, catalytic, and optical properties [1]. The main techniques for synthesizing nanoparticles are chemical, physical, and biological processes. Chemophysical approaches may result in energy waste and health issues, whereas the biological (green synthesis) approach is more economical, environmentally friendly, and safer for individuals [2]. In this method, nanoparticles were synthesized by bacteria, fungi, algae, and plants extracts [3].

Green synthesis, utilizing plant extracts, is favoured for its cost-effectiveness, accessibility, efficacy, and flexibility to use of different part of plants including, leaf, flower, fruit, root, stem, bark, seed, nut. Plants include many metabolites, including terpenoids, flavonoids, steroids, tannins, proteins, and starches, which encompass multiple functional groups and are capable of the reduction and prevent aggregation of NPs. Furthermore, nanoparticles synthesized using plant extract exhibit lower cytotoxicity [4].

Among metallic nanoparticles, AgNPs are recognized for their biological application including, antimicrobial, antioxidant, and anticancer properties [5]. Due to the increasing concern of antibiotic resistance, many researchers have turned their attention to silver nanoparticles because of their long-lasting antimicrobial effect on multidrug-resistant bacteria [6; 7]. Due to the diverse targets of silver nanoparticles, it is challenging for bacteria to evolve resistance mechanisms against them [1; 8]. Silver nanoparticles have gained significant importance as possible anticancer treatments due to their specific toxicity targeting cancer cells, as they alter cell shape, induce oxidative stress, and thus reduce cell viability [9].

Several research have revealed the medicinal properties of *Maranta leuconeura*, (family: Marantaceae) often known as the prayer plant. The concentration of chemical compounds like rutin in it makes these effects even more apparent [10]. *Maranta leuconeura* has many health benefits, and one of them is that it contains bioactive compounds, which boost its medicinal potential. To be more specific, rosmarinic acid extracts have garnered a lot of attention

because of the promising effects they may have in preventing and treating illnesses including cancer and atherosclerosis [11].

This is the first study to examine the ability of *Maranta leuconeura* ethanolic extract to synthesize AgNPs and assess their biological applications, including antibacterial efficacy against MDR bacteria, antioxidant activity measured by DPPH, and anticancer activity evaluated via MTT method against SiHa and HdFn cell lines.

Materials and methods

Preparation of *Maranta leuconeura* ethanolic leaf extract

The ethanolic leaf extract of *Maranta leuconeura* was prepared following the methodology of Swilam and Nematallah (2022) [12] with some modifications. The plant leaf was thoroughly rinsed with double distilled water, and then allowed to dry at room temperature in the shaded area. Following drying and grinding, the ethanolic extract was obtained by macerating 30 g of leaf powder in 1 L of 70% ethanol for 1 day at 30 °C. The extract was filtered through Whatman No. 1, then evaporated at 30°C.

Green synthesis of ML-AgNPs solution

The green synthesized solution of *Maranta leuconeura* AgNPs (ML-AgNPs), was prepared according to [13], by mixed 225 ml of 1 mM silver nitrate solution with 25 ml of 3% ethanolic leaves extract. ML-AgNPs solution were purified using centrifugation for 30 minutes at 4000 rpm to remove impurities. The pellets were then washed with deionized water, allowed to dry at ambient temperature, and then stored at 4°C.

Green synthesized ML-AgNPs characterization techniques

UV–Vis spectrum analysis

The initial conformation of the successful formation of ML-AgNPs was performed after color shift by using A UV-Visible spectrophotometer (Thermo, Biomate5) at the wave length of 250-800 nm.

Fourier transmission infrared spectroscopy (FTIR) analysis technique

The KBr technique, utilizing FTIR (ALPHA) at a spectral frequency of 4000–400 cm^{-1}, was employed for each dried plant extract and ML-AgNPs powder to identify the main functional groups responsible for NP reduction and capping.

X-ray diffraction (XRD) analysis of ML-AgNPs

The ML-AgNPs crystalline structures were confirmed by scanning the diffraction pattern with an X-ray diffractometer (PHLIPS, PW1730) from 20°C to 80°C in the 2θ range [14].

Zeta potential analyser

The HORIBA SZ-100 nanoparticle analyzer was utilized in this study to evaluate the stability of ML-AgNPs and to measure their surface charge.

FE-SEM and EDX analyses

FESEM (TESCAN, MIRA3) instrument was used for determined the particle size, and the morphological features of ML-AgNPs. The EDX analysis was conducted to identify the types of chemical elements in the ML-AgNPs sample and their respective percentages.

Antimicrobial activity of ML-AgNPs

Multidrug-resistant bacteria *(Staphylococcus epidermidis, Staphylococcus aureus, Escherichia coli, Shigella flexneri, Pseudomonas aeruginosa,* and *Proteus mirabilis*) obtained from Al-Fayha and Al-Sadar Teaching Hospitals in Basrah, were used to evaluate ML-AgNPs antimicrobial activity, by agar-well diffusion method. According to (Vijapur *et al.,* 2023) [15], with specific modifications, the bacterial suspension exhibiting 0.5 McFarland turbidity, spreader on plates with Muller-Hinton agar (MHA). Five 6-mm wells were formed. Each plate included a sterile cork borer. To obtain ML-AgNPs 500 µg/ml stock solution, 10 mg of ML-AgNPs powder was mixed with 20 ml of Dimethyl sulfoxide (DMSO). Subsequently, to each well, 100 µl of a two-fold serial dilution was added, with DMSO as a control. The plates were incubated at 37°C for 24 hours. The hollow zones around wells measured the inhibition of ML-AgNPs in millimeters.

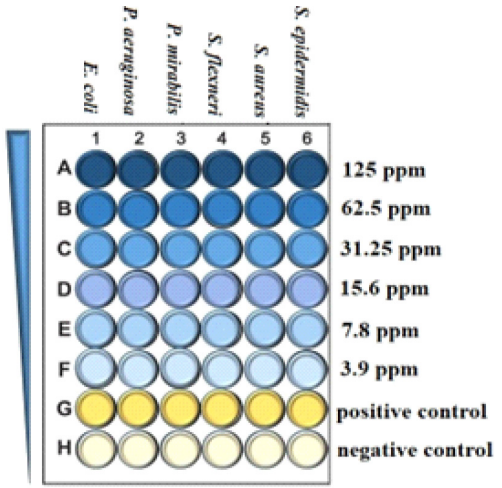

Fig. 1. Schematic of the MIC microtiter plates

Microdilution assays were conducted in 96-well microtiter plates for the minimum inhibitory concentration (MIC), following the CLSI (34th Ed.) procedure [16]. 2.5 ml of the stock solution (500 µg/ml) diluted with 7.5 ml of Muellar-Hinton broth (MHB) to obtain 125 µg/ml. which was used to prepare a serial dilution from 125 to 3.9 µg/ml. To each well in rows A to F, 100 µl of each concentration was added (Fig. 1). Wells in rows A-G for columns 2-5 were then treated with 20 µl of each bacterial suspension. In the last step, 100 µl of MHB was dispensed into the positive and negative control wells located in rows G and H respectively. The plate was incubated at 37°C for 24 hours.

To observe color change, 20 µl of purple resazurin dye solution with a concentration 0.016% was added and incubated for 2 hours. Color Pink or purple indicates bacterial growth, whereas color blue indicates inhibitory concentration. The MIC value represent the final well in a column without color change. By inoculating MHA plates with contents from the MIC well and the well with the highest concentration, the MBC was established.

Evaluation of ML-AgNPs cytotoxicity effect

ML-AgNPs were evaluated for cytotoxicity and antitumor efficacy against cervical cancer cell line (SiHa) and human dermal fibroblasts, neonatal normal cell line (HdFn) by the MTT assay. In 96-well microtiter plates, $1x10^4$ to $1x10^6$ cells/ml were inoculated with 200 µl of media and incubated for 24 hours at 37°C. Subsequently, 200 µl of ML-AgNPs various concentration (ranging from 400 to 25 µg/ml) were added and incubated for two days. Following exposure to ML-AgNPs, 10 µl of MTT solution was added to every well and left to incubate for four hours. The formazan blue crystals were dissolved by adding 100 µl of DMSO to each well after the media was carefully removed. The absorbance was measured at 575 nm using the ELISA reader (Bio-Rad, Germany). The cytotoxicity test was assessed by calculating the IC50 value, which represents the concentration exhibiting 50% inhibitory activity [17].

Antioxidant effect of synthesized ML-AgNPs

Following the methodology of [18], the antioxidant activity of ML-AgNPs was assessed using the DPPH method. A total of 500 µL of ML-AgNPs and ascorbic acid, diluted twofold serially from 200 to 12.5 µg/ml, was added to separate reaction tubes. Concurrently, each concentration was supplemented with 3000 µL of a 9:1 v/v mixture of methanol and DMSO, and 300 µL of a DPPH solution (0.1 mg/ml). The tubes were gently agitated for a few seconds and left in the absence of light for one hour at room temperature. Incubation was followed by absorption measurements at 517 nm using ELISA readers. The

methanol-DMSO mixture and DPPH solution were used as negative controls, while the ascorbic acid used as a reference.

Statistical analysis

Mean ± standard deviation was used for all research data. The antibacterial activity result was assessed using a one-way ANOVA analysis in SPSS, version 22 (IBM Company, Chicago, IL, USA). Significance differences were determined at a p-value ≤ 0.05. Graph Pad Prism 10.4.0 was used to analyze anticancer and antioxidant findings, whereas Origin Pro 10.15 displayed FTIR and XRD data.

Result and discussion

Green synthesis of ML-AgNPs solution

In this eco-friendly method, ML-AgNPs were produced by mixing plant extract with $AgNO_3$ solution. (Fig. 2) demonstrates that after 5 days at room temperature, the reaction solution's color changes from light brown to dark brown. This clearly supports the synthesis of ML-AgNPs. The color change in the silver nanoparticle solution was caused by surface plasmon resonance (SPR), which proved that the secondary metabolites in the plant extract reduced the silver ions. Previous research varied in their assessment of the duration needed for the AgNPs solution to change color. Some reported that the initial color change in medicinal plants occurred within 1 to 4 hours, while others reported it within 3 days to 14 days in non-medicinal plants. This discrepancy is due to the the difference in concentration of bioactive compound, which are crucial to NPs synthesis [19].

Fig. 2. Color shift of the reaction mixture

Green synthesized ML-AgNPs characterization techniques

UV–Vis spectrum analysis

After the visible color change, the synthesis of ML-AgNPs was confirmed using this simple, efficient, and very sensitive method. A single narrow absorp-

tion peak at 400 nm characterizes the UV-vis absorption spectra of AgNPs, as seen in Fig. 3. The SPR absorption band occurs when silver nanoparticles are exposed to light waves due to the proximity of their conduction and valence bands, facilitating collective electron oscillation in resonance. The absorbance is influenced by the chemical environment, nanoparticle dimensions and morphology, dielectric medium, and nanoparticle configuration [20]. The distinctive band of spherical AgNPs, according to [21], typically peaks between 400 and 420 nm. The relationship between SPR absorption band and shape is corroborated by SEM research on ML-AgNPs. Numerous studies have documented an absorption peak between 400 and 450 nm, including [22] study, which identified the SPR peak at 400 nm.

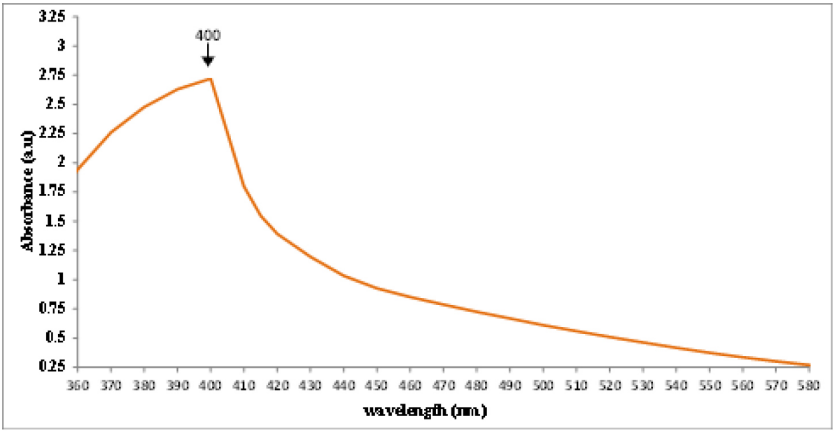

Fig. 3. UV-Visible spectrum of biosynthesis ML-AgNPs

Fourier transmission infrared (FTIR) spectroscopy analysis technique

To determine the plant biomolecule functional groups that reduced silver ions into AgNPs, FTIR analysis was performed. Fig. 4 shows the FTIR spectra for both the *Maranta leuconeura* extract and the ML-AgNPs.

The FTIR spectrum of the plant extract shows multiple peaks, with the most prominent ones being 3352.2 cm^{-1} for the stretching of the O−H group in alcohols and phenolic compounds, 2976.3 cm^{-1} for the stretching of the C−H group in alkanes, 2897.2 cm^{-1} for the stretching of the O−H group in alcohol, 1732.8 cm^{-1} for the C−H bending of aromatic compounds, and 1644.0 cm^{-1} for the C=C stretching vibrations of the alkene functional groups [23]. The FTIR spectrum of the AgNPs was similar to that of the plant extract with slight shift

in the positions of peaks as well as the disappearance of other peaks which indicates the successful synthesis of silver nanoparticles. The O-H stretching vibrations of the phenolic functional and alcoholic groups were identified at 3436.9 cm^{-1} as a wide peak.

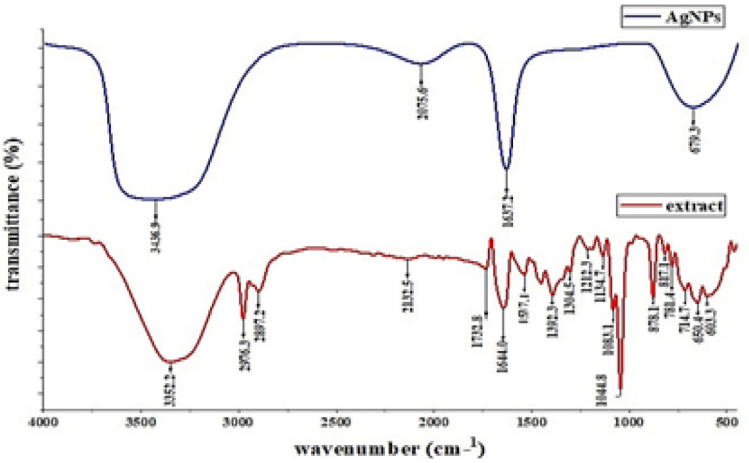

Fig. 4. ML-AgNPs with *Maranta leuconeura* ethanolic leaf extract FTIR spectrum

The alkene functional group's C=C stretching cause the 1636 cm-1 band. The band at 679 cm-1 indicates a link between silver nanoparticles and hydroxyl group oxygen [24]. The AgNPs spectrum shows these functional groups, notably in the 1600-1700 cm^{-1} region, confirming their significance in reducing silver ions to silver nanoparticles and producing a coating layer on their surface to avoid aggregation [25; 26].

X-ray diffraction (XRD) analysis of ML-AgNPs

The findings validated the sample's crystalline characteristics and showed that the silver had a cubic crystalline structure (Fig. 5), as indicated by reference code 96-901-1667. The following 2θ angles showed the principal diffraction peaks: 27.9°, 32.3°, 46.4°, 55.0°, 57.8°, 67.5°, 74.4°, and 77.1°. The crystal planes (111), (200), (220), (311), (222), (400), (311), and (410), respectively, are represented by these peaks. While the larger peaks might suggest some particle size fluctuation, the sharpness of these peaks suggests good crystallinity, the peak at 2θ of 32.38° seems to be associated with silver oxide, while of 27.99° may correspond to the bioorganic compound from *Maranta leuconeura* leaf that act as capping agent of AgNPs [27].

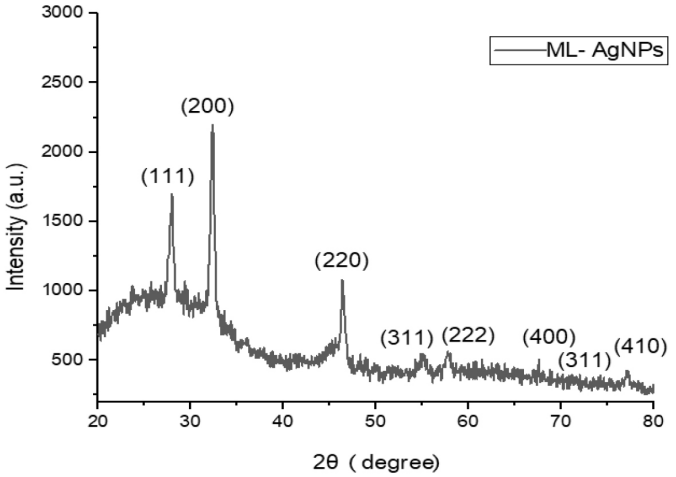

Fig. 5. XRD pattern of the synthesized ML-AgNPs

Zeta potential analyzer

The zeta potential analyzer was used to measure the surface electrical charge to evaluate synthesized nanoparticles stability. Fig. 6 shows that the ML-AgNPs surface in the colloidal solution had a negative charge of -37.1 mV (Fig. 6).

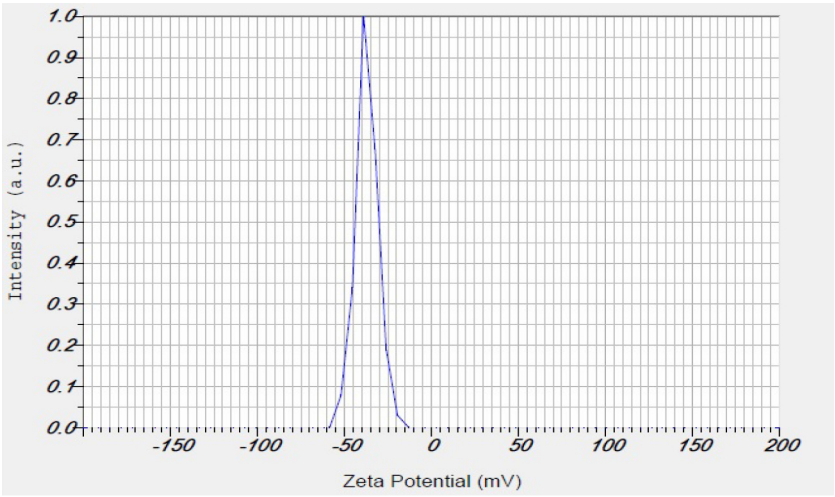

Fig. 6. Green synthesised ML-AgNPs zeta potential analysis

According to [28], the high stability, as shown by a zeta potential value above +30 mV or below −30 mV, is enhanced by particle repulsion. FTIR investigations indicate that the hydroxyl functional groups, which stabilize AgNPs and inhibit aggregation, can be responsible for the negative electrical charge [29].

FE-SEM and EDX analyses

The particles sizes and shape of silver nanoparticles were revealed by the FE-SEM investigation. The biosynthetic ML-AgNPs had an almost homogeneous, spherical in shape and an average diameter of 39.9 ± 5.4 nm at 120000 x magnification, as shown in (Fig. 7) of the FESEM image. The size distribution histogram indicated that the ML-AgNPs size range, approximately between 25 and 55 nm. This narrow size distribution indicates the efficacy of plant extract to produce homogeneous size and shape of ML-AgNPs which is crucial for their activities. Researchers vary in their assessment of the size and morphology of silver nanoparticles, and this variation is attributable to the experimental conditions and reduction agent [30].

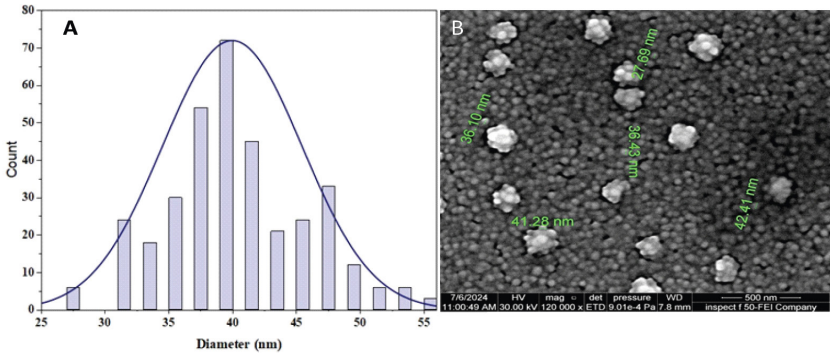

Fig. 7. (A) Size distribution histogram of ML-AgNPs (B) FESEM image of biosynthesis ML-AgNPs

The elemental composition of ML-AgNPs was investigated using EDX spectroscopy. The presence of silver nano crystallites is confirmed by the spectra's high signal peak at around 3 keV (Fig. 8), which indicates a silver element with a high weight percentage of 71.87% [31]. In contrast, the presence of Cl, O, and Ca is indicated by weak signals at 18.55%, 8.54%, and 1.04% weight percentages, respectively. These elements might be present because of the surface biomolecules that capped the ML-AgNPs or could be appear as a result for preparing sample to analysis by FESEM instrument.

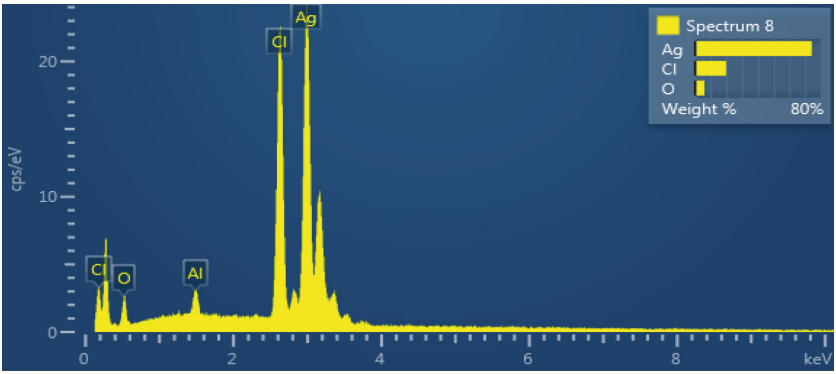

Fig. 8. EDX spectrum analysis of biosynthesized ML- AgNPs

Antimicrobial activity of ML-AgNPs

The ability of ML-AgNPs to inhibit six multidrug-resistant pathogenic bacteria growth shown in Fig. 9. According to the result presented in Table 1, it was clear that *S. epidermidis* and *P. mirabilis* were the most significantly sensitive isolates to ML-AgNPs with 14.4 mm inhibition zone, while *S. aureus* was the lowest sensitive isolates to silver nanoparticle at 12.8 mm of inhibition zone. The highest concentration demonstrated the greatest activity against all tested isolates, whereas the lowest effectiveness of AgNPs was observed at 62.5 µg/ml; this finding is consistent with prior research, including that of [32].

Table 1.

Inhibition zones diameter of tested bacterial isolates by various concentrations of ML-AgNPs

Bacterial isolates	ML-AgNPs Concentration (µg/ml)				Total mean
	500	250	125	62.5	
P. aeruginosa	15 ± 0.49	13 ± 0.55	13 ± 0.51	12 ± 0.10	13.4 ± 1.48 ^{a}
E. coli	15 ± 0.52	14 ± 0.43	13 ± 0.49	12 ± 0.66	13.8 ± 0.95 ^{ab}
P. mirabilis	15 ± 0.55	15 ± 0.51	14 ± 0.10	13 ± 0.49	14.4 ± 0.75 ^{bc}
S. flexneri	15 ± 0.60	14 ± 0.10	14 ± 0.15	12 ± 0.55	13.8 ± 0.96 ^{abcd}
S. aureus	14 ± 0.49	13 ± 0.55	12 ± 0.05	11 ± 0.46	12.8 ± 1.31 ^{ae}
S. epidermidis	15 ± 0.60	15 ± 0.15	14 ± 0.51	13 ± 0.60	14.4 ± 0.68 ^{bcd}
Total mean	15 ± 0.64 ^{a}	14 ± 0.67 ^{b}	13 ± 0.91 ^{c}	12 ± 0.95 ^{d}	13.7 ± 1.16
- distinct letters indicating significant variations at $p \leq 0.05$					

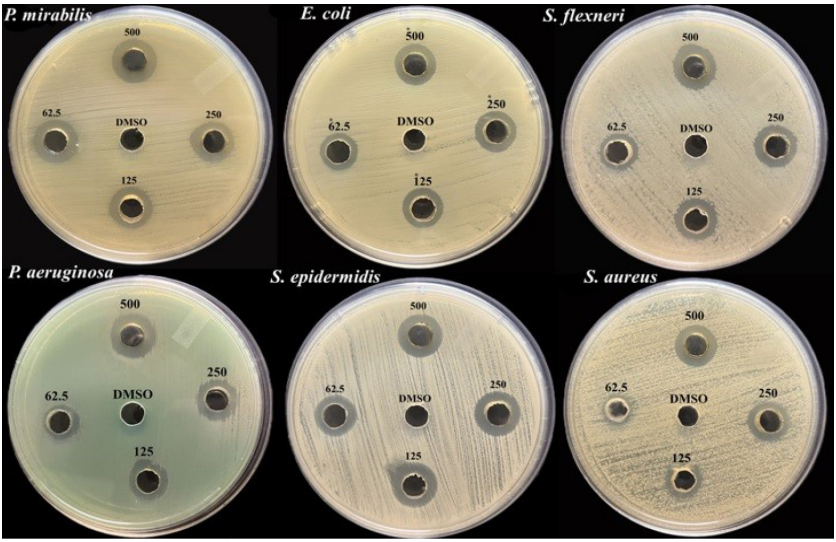

Fig. 9. Antibacterial activity of ML-AgNPs against MDR-bacteria

Table 2 shows the resazurin-based microtiter dilution technique used to determine these isolates' MIC and MBC values. The MIC value was 125 µg/ml for Gr+ bacterial isolates and 62.5 µg/ml for Gr- bacterial isolates. At 125 µg/ml, *S. aureus, S. epidermidis*, and *E. coli* had the lowest MBC findings, whereas *P. aeruginosa, P. mirabilis, and S. flexneri* recorded the highest MBC values at 62.5 µg/ml. The thin peptidoglycan layer of Gr- bacteria cell walls facilitate the penetration of nanoparticles, even at lower concentrations, hence suppressing bacterial growth. This may clarify why their MIC values are lower than those of Gr+ bacteria.

Table 2.

MIC and MBC values tested MDR-isolates

MDR bacteria		MIC value (µg/ml)	MBC value (µg/ml)
Gram-negative bacteria	*P. aeruginosa*	62.5	62.5
	E. coli	62.5	125
	P. mirabilis	62.5	62.5
	S. flexneri	62.5	62.5
Gram-positive bacteria	*S. aureus*	125	125
	S. epidermidis	125	125

The exact process by which silver nanoparticles exert their antibacterial effects is still not fully understood. Researchers propose that the binding of silver nanoparticles to the plasmic membrane damages selective permeability, disrupts respiratory chain enzymes, causes leakage of subcellular components or induces oxidative stress by free radical formation [33; 34].

Evaluation of ML-AgNPs cytotoxicity effect

The potential anticancer and cytotoxic effects of ML-AgNPs were shown by the MTT assay on the HdFn normal cell line and the SiHa cancer cell line, with dosages ranging from 400 to 25 µg/ml. The concentration-dependent inhibition of SiHa and HdFn was seen after 24 hours of exposure to ML-AgNPs, as shown in Fig. 10. The IC_{50} for SiHa was 17.49 µg/ml, while the IC50 for HdFn was 125 µg/ml. These significant differences indicate the anticancer potential of ML-AgNPs. It was obvious that cancer cells were more susceptible to silver nanoparticles than normal cells.

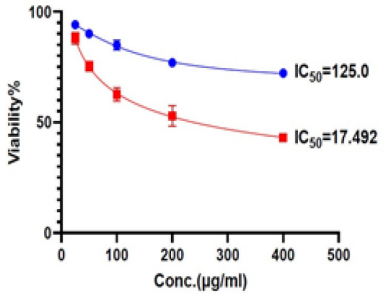

Concentration µg/ml	SiHa (mean+SD)	HdFn (mean+SD)
400	43.05 ± 1.7	72.18 ± 1.6
200	52.85 ± 4.6	76.96 ± 1.4
100	62.65 ± 3.0	84.83 ±2.3
50	75.34 ± 2.2	90.04 ± 1.2
25	87.92 ± 2.4	94.13 ± 1.3

Fig. 10. Cytotoxicity effect of ML-AgNPs

[35] suggest that NPs sized between 10 and 100 nm exhibit less toxicity to normal cells while demonstrating significant toxicity to cancer cells. This indicates that the diameter of the nanoparticles produced in the present study (39.9 nm), as demonstrated by SEM, may have significantly influenced the anticancer effectiveness, or that cancer cells possess an enhanced ability for the cellular uptake of AgNPs. The proposed mechanism of action of biosynthesized nanoparticles on the cervical cancer line, indicated increased ROS generation, cell morphological alterations, and DNA fragmentation that ends in cell death [36]. Several research indicated AgNPs anticancer effect on SiHa cell line such as [37] with an IC_{50} of 18.25 µg/ml, which is comparable to the current study, while other studies have reported different IC50 values including [38] and [39]. This variance may be attributable to cell line type, size, shape and NP surface charge.

Antioxidant effect of synthesized ML-AgNPs

The activities of ML-AgNPs in scavenging free radicals at various concentrations (200, 100, 50, 25 µg/ml) and ascorbic acid as a reference are shown in Fig. 11 and Table 3. The antioxidant activity of AgNPs increased with concentration, confirming their scavenging effect. At all concentrations the scavenging ability of ML-AgNPs was close to the standard, with no significant differences except for 12.5 µg/ml, where it higher than ascorbic acid. The highest scavenging percentage of ML-AgNPs was measured at 200 µg/mL, which was 73.34 ± 1.39 %. This value was greater than the results obtained at the same concentration from [40] (62.22%) and [41] (64.9%).

Table 3.

Effects of AgNPs and ascorbic acid on DPPH radical scavenging

Tested Concentration µg/ml	Scavenging percent (%)	
	ML-AgNPs (mean ±SD)	Ascorbic acid (mean ±SD)
200	73.34 ± 1.3	77.23 ± 2.4
100	64.77 ± 1.4	66.43 ± 0.9
50	52.70 ± 3.2	55.05 ± 1.5
25	42.70 ± 1.8	43.51 ± 0.8
12.5	28.39 ± 0.6	26.11 ± 0.2

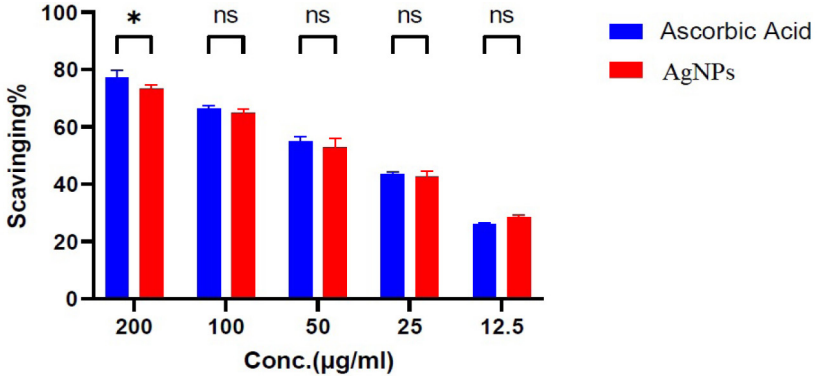

Fig. 11. Free radical scavenging ability of ML-AgNPs and ascorbic acid

[42] proposed that the antioxidant effect of AgNPs caused by the simultaneous action of polyphenols, and the nanoparticles themselves, which function as catalysts, this may explain the capacity of ML-AgNPs, coated by polyphenols (as shown by FTIR spectrum), to scavenge free radicals.

Conclusions

This safe and economical approach effectively synthesized AgNPs, utilizing ethanolic extract of *Maranta leuconeura* leaves. The biosynthesized ML-AgNPs were spherical, nanoscale, non-aggregated, pure, and showed a long term of stability. They demonstrated efficacy against Gr- and Gr+ bacteria, and showed good antioxidant activity close to the ascorbic acid. The present study also revealed distinct cytotoxicity against SiHa cancer cells. Additional in vitro studies are necessary to evaluate cancer cell targeting methodologies.

References

1. Singh, A., Gautam, P. K., Verma, A., Singh, V., Shivapriya, P. M., Shivalkar, S., Sahoo, A. K., & Samanta, S. K. (2020). Green synthesis of metallic nanoparticles as effective alternatives to treat antibiotics resistant bacterial infections: A review. *Biotechnology Reports*, *25*, 1-13. https://doi.org/10.1016/j.btre.2020.e00427 EDN: https://elibrary.ru/BSVIFJ
2. Ying, S., Guan, Z., Ofoegbu, P. C., Clubb, P., Rico, C., He, F., & Hong, J. (2022). Green synthesis of nanoparticles: Current developments and limitations. *Environmental Technology & Innovation*, *26*, 1-20.
3. Arif, R., & Uddin, R. (2021). A review on recent developments in the biosynthesis of silver nanoparticles and its biomedical applications. *Medical Devices & Sensors*, *4*(1), 1-20.
4. Paiva-Santos, A. C., Herdade, A. M., Guerra, C., Peixoto, D., Pereira-Silva, M., Zeinali, M., Mascarenhas-Melo, F., Paranhos, A., & Veiga, F. (2021). Plant-mediated green synthesis of metal-based nanoparticles for dermopharmaceutical and cosmetic applications. *International Journal of Pharmaceutics*, *597*, 1-10. https://doi.org/10.1016/j.ijpharm.2021.120311 EDN: https://elibrary.ru/LURTJC
5. Sharma, B., Singh, I., Bajar, S., Gupta, S., Gautam, H., & Kumar, P. (2020). Biogenic silver nanoparticles: Evaluation of their biological and catalytic potential. *Indian Journal of Microbiology*, *60*, 468-474. https://doi.org/10.1007/s12088-020-00889-0 EDN: https://elibrary.ru/TXQPEC
6. Khan, S. A., Shahid, S., & Lee, C. S. (2020). Green synthesis of gold and silver nanoparticles using leaf extract of *Clerodendrum inerme*; characterization, antimicrobial, and antioxidant activities. *Biomolecules*, *10*, 835-865. https://doi.org/10.3390/biom10060835 EDN: https://elibrary.ru/ORGNHP
7. AlKhafaji, M. H., Mohsin, R. H., & Faqri, A. M. A. (2024). Food Additive Mediated Biosynthesis of AgNPs with Antimicrobial Activity Against Hypermucoviscous Enterotoxigenic Foodborne *Klebsiella pneumoniae*. *Basrah Journal of Agricultural Sciences*, *37*(1), 278-295. https://doi.org/10.37077/25200860.2024.37.1.21 EDN: https://elibrary.ru/XGOOMR

8. Fatima, A., Shehzad A., Shahzad R., Khan S., Al-Suhaimi E.A. (2024). Impact of nanoparticles on structural elements within the cells. In *Molecular impacts of nanoparticles on plants and algae* (pp. 111-141). Cambridge, US: Academic Press.
9. Ratan, Z. A., Haidere, M. F., Nurunnabi, M. D., Shahriar, S. M., Ahammad, A. S., Shim, Y. Y., Reaney, M. J. T., & Cho, J. Y. (2020). Green chemistry synthesis of silver nanoparticles and their potential anticancer effects. *Cancers*, *12*(4), 855-881. https://doi.org/10.3390/cancers12040855 EDN: https://elibrary.ru/LGYCNB
10. Habtemariam, S., & Varghese, G. K. (2015). Extractability of rutin in herbal tea preparations of *Moringa stenopetala* leaves. *Beverages*, *1*(3), 169-182.
11. Amoah, S. K., Sandjo, L. P., Kratz, J. M., & Biavatti, M. W. (2016). Rosmarinic acid-pharmaceutical and clinical aspects. *Planta Medica*, *82*(5), 388-406. https://doi.org/10.1055/s-0035-1568274 EDN: https://elibrary.ru/UNJOEO
12. Swilam, N., & Nematallah, K. A. (2020). Polyphenols profile of pomegranate leaves and their role in green synthesis of silver nanoparticles. *Scientific Reports*, *10*(1), 1-11. https://doi.org/10.1038/s41598-020-71847-5 EDN: https://elibrary.ru/JLNOXK
13. Reddy, N. V., Li, H., Hou, T., Bethu, M. S., Ren, Z., & Zhang, Z. (2021). Phytosynthesis of silver nanoparticles using *Perilla frutescens* leaf extract: characterization and evaluation of antibacterial, antioxidant, and anticancer activities. *International Journal of Nanomedicine*, *16*, 15-29.
14. Weeranantanapan, O., Chudapongse, N., Limphirat, W., & Nantapong, N. (2022). *Streptomyces chiangmaiensis* SSUT88A mediated green synthesis of silver nanoparticles: Characterization and evaluation of antibacterial action against clinical drug-resistant strains. *RSC Advances*, *12*, 4336-4345. https://doi.org/10.1039/d1ra08238h EDN: https://elibrary.ru/HXCGDV
15. Vijapur, L. S., Srinivas, Y., Desai, A. R., Gudigennavar, A. S., Shidramshettar, S. L., & Yaragattimath, P. (2023). Development of biosynthesized silver nanoparticles from *Cinnamomum tamala* for anti-oxidant, anti-microbial and anti-cancer activity. *Journal of Research in Pharmacy*, *27*(2), 769-782.
16. CLSI. (2024). *Performance standards for antimicrobial susceptibility testing, M100*, 34th ed. US: Clinical and Laboratory Standards Institute.
17. Hussein, A. A., Albarazanchi, S. I., & Al-Shanon, A. F. (2020). Evaluation of anticancer potential for L-glutaminase purified from *Bacillus subtilis*. *International Journal of Pharmaceutical Research*, *12*(1), 293–299.
18. Al-Saffar, A. Z., Al-Shanon, A. F., Al-Brazanchi, S. L., Sabry, F. A., Hassan, F., & Hadi, N. A. (2017). Phytochemical analysis, antioxidant and cytotoxic

potentials of *Pelargonium graveolens* extract in human breast adenocarcinoma (MCF-7) cell line. *Asian Journal of Biochemistry*, *12*(1), 16-26.

19. Urnukhsaikhan, E., Bold, B. E., Gunbileg, A., Sukhbaatar, N., & Mishig-Ochir, T. (2021). Antibacterial activity and characteristics of silver nanoparticles biosynthesized from *Carduus crispus*. *Scientific Reports*, *11*(1), 1-12. https://doi.org/10.1038/s41598-021-00520-2 EDN: https://elibrary.ru/WAGIAC
20. Salleh, A., Naomi, R., Utami, N. D., Mohammad, A. W., Mahmoudi, E., Mustafa, N., & Fauzi, M. B. (2020). The potential of silver nanoparticles for antiviral and antibacterial applications: A mechanism of action. *Nanomaterials*, *10*(8), 1566-1586. https://doi.org/10.3390/nano10081566 EDN: https://elibrary.ru/TCWRJZ
21. Raja, S., Ramesh, V., & Thivaharan, V. (2017). Green biosynthesis of silver nanoparticles using *Calliandra haematocephala* leaf extract, their antibacterial activity and hydrogen peroxide sensing capability. *Arabian Journal of Chemistry*, *10*, 253–261.
22. Abdulsahib, S. S. (2021). Synthesis, characterization and biomedical applications of silver nanoparticles. *Biomedicine*, *41*(2), 458-464. https://doi.org/10.51248/.v41i2.1058 EDN: https://elibrary.ru/DTUPFA
23. Sharifi-Rad, M., Pohl, P., & Epifano, F. (2021). Phytofabrication of silver nanoparticles (AgNPs) with pharmaceutical capabilities using *Otostegia persica* (Burm.) Boiss. leaf extract. *Nanomaterials*, *11*(4), 1045-1063. https://doi.org/10.3390/nano11041045 EDN: https://elibrary.ru/RZCTAX
24. Said, A., Abu-Elghait, M., Atta, H. M., & Salem, S. S. (2024). Antibacterial activity of green synthesized silver nanoparticles using *Lawsonia inermis* against common pathogens from urinary tract infection. *Applied Biochemistry and Biotechnology*, *196*(1), 85-98. https://doi.org/10.1007/s12010-023-04482-1 EDN: https://elibrary.ru/CXJVUY
25. Mohammadi, S., Pourseyedi, S., & Amini, A. (2016). Green synthesis of silver nanoparticles with a long lasting stability using colloidal solution of cowpea seeds (*Vigna* sp. L). *Journal of Environmental Chemical Engineering*, *4*(2), 2023-2032. https://doi.org/10.1016/j.jece.2016.03.026 EDN: https://elibrary.ru/WVCOSR
26. Chand, K., Cao, D., Fouad, D. E., Shah, A. H., Dayo, A. Q., Zhu, K., Lakhan, M. N., Mehdi, G., & Dong, S. (2020). Green synthesis, characterization and photocatalytic application of silver nanoparticles synthesized by various plant extracts. *Arabian Journal of Chemistry*, *13*(11), 8248-8261. https://doi.org/10.1016/j.arabjc.2020.01.009 EDN: https://elibrary.ru/VUOGGA
27. Gevorgyan, S., Schubert, R., Falke, S., Lorenzen, K., Trchounian, K., & Betzel, C. (2022). Structural characterization and antibacterial activity of silver

nanoparticles synthesized using a low-molecular-weight Royal Jelly extract. *Scientific Reports*, *12*(1), 1-12. https://doi.org/10.1038/s41598-022-17929-y EDN: https://elibrary.ru/YEMCEQ

28. Nagaraja, S., Ahmed, S. S., DR, B., Goudanavar, P., Fattepur, S., Meravanige, G., Shariff, A., Shiroorkar, P. N., Habeebuddin, M., & Telsang, M. (2022). Green synthesis and characterization of silver nanoparticles of *Psidium guajava* leaf extract and evaluation for its antidiabetic activity. *Molecules*, *27*(14), 1-12. https://doi.org/10.3390/molecules27144336 EDN: https://elibrary.ru/HCTIUU
29. Wan Mat Khalir, W. K. A., Shameli, K., Jazayeri, S. D., Othman, N. A., Che Jusoh, N. W., & Hassan, N. M. (2020). Biosynthesized silver nanoparticles by aqueous stem extract of *Entada spiralis* and screening of their biomedical activity. *Frontiers in Chemistry*, *8*, 620-635.
30. Velgosova, O., Mačák, L., Čižmárová, E., & Mára, V. (2022). Influence of reagents on the synthesis process and shape of silver nanoparticles. *Materials*, *15*(19), 1-10. https://doi.org/10.3390/ma15196829 EDN: https://elibrary.ru/CLTUTY
31. Akter, S., Lee, S. Y., Siddiqi, M. Z., Balusamy, S. R., Ashrafudoulla, M., Rupa, E. J., & Huq, M. A. (2020). Ecofriendly synthesis of silver nanoparticles by *Terrabacter humi* sp. nov. and their antibacterial application against antibiotic-resistant pathogens. *International Journal of Molecular Sciences*, *21*(24), 1-19.
32. Shareef, A. A., Hassan, Z. A., Kadhim, M. A., & Al-Mussawi, A. A. (2022). Antibacterial Activity of Silver Nanoparticles Synthesized by Aqueous Extract of *Carthamus oxycantha* M. Bieb. Against Antibiotics Resistant Bacteria. *Baghdad Science Journal*, *19*(3), 460-468. https://doi.org/10.21123/BSJ.2022.19.3.0460 EDN: https://elibrary.ru/HDLJFK
33. Aref, M. S., & Salem, S. S. (2020). Bio-callus synthesis of silver nanoparticles, characterization, and antibacterial activities via *Cinnamomum camphora* callus culture. *Biocatalysis and Agricultural Biotechnology*, *27*. https://doi.org/10.1016/j.bcab.2020.101689 EDN: https://elibrary.ru/KZJPMQ
34. Elakraa, A. A., Salem, S. S., El-Sayyad, G. S., & Attia, M. S. (2022). Cefotaxime incorporated bimetallic silver-selenium nanoparticles: promising antimicrobial synergism, antibiofilm activity, and bacterial membrane leakage reaction mechanism. *RSC Advances*, *12*(41), 26603-26619. https://doi.org/10.1039/d2ra04717a EDN: https://elibrary.ru/WGFIIV
35. Sukhanova, A., Bozrova, S., Sokolov, P., Berestovoy, M., Karaulov, A., & Nabiev, I. (2018). Dependence of nanoparticle toxicity on their physical and chemical properties. *Nanoscale Research Letters*, *13*, 1-21. https://doi.org/10.1186/s11671-018-2457-x EDN: https://elibrary.ru/XYCZJR

36. Pucelik, B., Sułek, A., Borkowski, M., Barzowska, A., Kobielusz, M., & Dąbrowski, J. M. (2022). Synthesis and characterization of size-and charge-tunable silver nanoparticles for selective anticancer and antibacterial treatment. *ACS Applied Materials & Interfaces*, *14*(13), 14981-14996. https://doi.org/10.1021/acsami.2c01100 EDN: https://elibrary.ru/WSSINJ
37. Mohammed Asik, R., Manikkaraja, C., Tamil Surya, K., Suganthy, N., Priya Aarthy, A., Mathe, D., Sivakumar, M., Archunan, G., & Padmanabhan, P., Gulyas, B. (2021). Anticancer Potential of L-Histidine-Capped Silver Nanoparticles against Human Cervical Cancer Cells (SiHA). *Nanomaterials*, *11*(11), 3154-3171. https://doi.org/10.3390/nano11113154 EDN: https://elibrary.ru/EQLPXQ
38. Tripathi, D., Modi, A., Smita, S. S., Narayan, G., & Pandey-Rai, S. (2022). Biomedical potential of green synthesized silver nanoparticles from root extract of *Asparagus officinalis*. *Journal of Plant Biochemistry and Biotechnology*, *31*(1), 213-218.
39. Gowda, A. T. C. S., Anil, V. S., & Raghavan, S. (2024). Phytosynthesis of silver nanoparticles using aqueous sandalwood (*Santalum album* L.) leaf extract: Divergent effects of SW-AgNPs on proliferating plant and cancer cells. *PLOS ONE*, *19*(4), 1-32.
40. Subramanyam, G. K., Gaddam, S. A., Kotakadi, V. S., Palithya, S., Penchalaneni, J., & Challagundla, V. N. (2021). *Argyreia nervosa* (Samudra pala) leaf extract mediated silver nanoparticles and evaluation of their antioxidant, antibacterial activity, in vitro anticancer and apoptotic studies in KB oral cancer cell lines. *Artificial Cells, Nanomedicine, and Biotechnology*, *49*(1), 634-649. https://doi.org/10.1080/21691401.2021.1996384 EDN: https://elibrary.ru/PGOFBV
41. Palle, S. R., Penchalaneni, J., Lavudi, K., Gaddam, S. A., Kotakadi, V. S., & Challagundala, V. N. (2020). Green synthesis of silver nanoparticles by leaf extracts of *Boerhavia erecta* and spectral characterization and their antimicrobial, antioxidant and cytotoxic studies on ovarian cancer cell lines. *Letters in Applied NanoBioScience*, *9*(3), 1165-1176. https://doi.org/10.33263/lianbs93.11651176 EDN: https://elibrary.ru/OOAEQA
42. Khorrami, S., Zarrabi, A., Khaleghi, M., Danaei, M., & Mozafari, M. R. (2018). Selective cytotoxicity of green synthesized silver nanoparticles against the MCF-7 tumor cell line and their enhanced antioxidant and antimicrobial properties. *International Journal of Nanomedicine*, *13*, 8013-8024.

DATA ABOUT THE AUTHORS

Noor M. Alassadi, MSc. Student, Department of Biology
College of Education for Pure Sciences, University of Basrah
Basrah, Iraq

nooralassadi887@gmail.com
ORCID: https://orcid.org/0009-0006-0700-2852

Ghaida'a J. Al-Ghizzawi, PhD, Prof., Department of Biology
College of Education for Pure Sciences, University of Basrah
Basrah, Iraq
ORCID: https://orcid.org/0000-0003-0533-1143
ghaeda.abdulnabi@uobasrah.edu.iq

Поступила 20.02.2024
После рецензирования 01.04.2024
Принята 27.05.2024

Received 20.02.2024
Revised 01.04.2024
Accepted 27.05.2024